ANALYTICAL STUDY OF RGB VERTICAL STRIPE AND RGBX SQUARE-SHAPED SUBPIXEL ARRANGEMENTS

Lu Fang ⋆*, Oscar C. Au* †*, Jingjing Dai* †*, Hanli Wang* ‡*, Ngai-Man CHEUNG* ⋆

⋆ Singapore Univ. of Tech. and Design, Singapore
† Hong Kong Univ. of Sci. and Tech., Hong Kong
‡ Tongji University, Shanghai, China

ABSTRACT

The frequency characteristics of subpixel-based decimation with RGB vertical stripe and RGBX square-shaped subpixel arrangements are studied. To achieve higher apparent resolution than pixel-based decimation, the sampling locations are specially chosen for each of two subpixel arrangements, resulting in relatively small magnitudes of horizontal and vertical aliasing spectra in frequency domain. Thanks to 2-D RGBX square-shaped subpixel arrangement, all the horizontal, vertical, diagonal and anti-diagonal aliasing spectra merely contain low-frequency information, indicating that subpixel-based decimation with RGBX square-shaped panel is more effective in retaining original high frequency details than RGB vertical stripe subpixel arrangement.

I. INTRODUCTION

A single pixel on a color LCD is composed by several (typically three) individual color elements ordered (on various displays) either as blue, green, and red (BGR), or as red, green, and blue (RGB). Some displays may have more than three primaries, often called Multi-Primary, such as the combination of red, green, blue, and yellow (RGBY), or red, green, blue, and white (RGBW). These colored primaries, sometimes called subpixels, are fused together to appear as a single color to human due to the blurring by the optics and spatial integration by nerve cells in the human eyes [1] [2]. Previously, simple pixel-based font display was used and the smallest level of detail that a computer could display on an LCD was a single pixel. However, researchers found that by controlling subpixel values of neighboring pixels, the number of points that may be independently addressed to reconstruct the image is increased, and it is possible to micro-shift the apparent position or orientation of a line (such as the edge of a font) by one or two subpixel width [3]. Methods that take this interaction between the display technology and the human visual system into account are called subpixel rendering algorithms [2].

About 20 years ago, the Apple II personal computer introduced a proprietary high resolution LCD graphics display in which each pixel has two vertical stripe subpixels with green and magenta colors respectively. The system controlled the individual subpixels in such a way that it could display fonts with better details than pixel-based rendering displays. Later, in 1998, Microsoft announced a subpixel-based font display technology called 'ClearType', which is a software technology capable of improving the readability of text on regular LCD with three RGB vertical stripe subpixels [1]. With ClearType running on an LCD monitor, features of text as small as a fraction of a pixel in width can be displayed. Fig. 1 illustrates an example of displaying the letter "m" with pixel rendering and ClearType, where ClearType can reduce staircase artifacts effectively and reconstruct the shape information more faithfully. However, subpixel rendering may cause local color imbalance called 'color fringing artifact' [2] [4], because, for some pixels, only one or two subpixels are turned on/off, as shown in Fig. 1-(c).

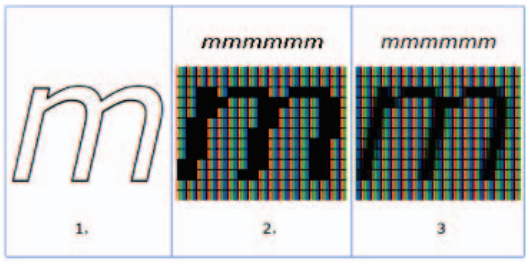

Fig. 1. (1) letter "m" in italic, (2) whole-pixel rendered "m" with jagged edges, (3) subpixel rendered "m" with smooth edges.

In LCDs that are mostly used to display edges/rectangles, the subpixels would be typically arranged in vertical stripe. Nevertheless, for the display of motion pictures, companies would tend to arrange subpixels in 2-D patterns so that the image variation is perceived better by viewers [5]. VP (Visual Perception) Dynamics developed a new 2-D VPW panel [6], where they modified LCD panel such that a regular RGB vertical stripe pixel is replaced by a VPW pixel with 4 square-shaped subpixels corresponding to red, green, blue and white color (RGBW), as shown in Fig. 2(b). Intuitively, VPW technology increases vertical apparent resolution by $2\times$ compared to RGB vertical stripe subpixel arrangement.

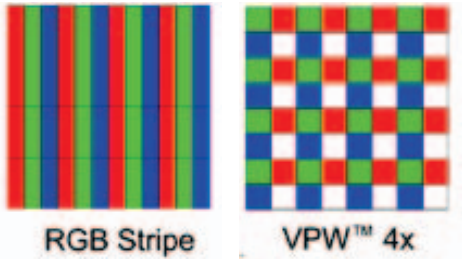

(a) (b)

Fig. 2. (a) Pixel geometry of RGB vertical stripe display (b) VPW (with RGBW subpixel/pixel) subpixel arrangement.

In this paper, we study and compare the frequency behavior of RGB vertical stripe and 2-D RGBX square-shaped subpixel arrangements. Note that X can be any color component (i.e., White or Yellow) except R, G, and B. Section II shows the detail of frequency analysis and comparison. Section III concludes the paper.

II. ANALYTICAL STUDY OF DIFFERENT SUBPIXEL ARRANGEMENTS

A major application of subpixel rendering is displaying high-resolution image on low-resolution display terminals, in which case, subpixel-based decimation that make use of RGB stripe or other dedicated subpixel arrangements achieve superior sharpness of down-sampled images [4]. As one pixel in conventional RGB stripe panel contains three subpixels, there exists natural decimation pattern for $3:1$ decimation. While the RGBX square-shaped panel repeats itself for every 2×2 block, so that the natural decimation pattern exists for $2:1$ decimation. Without loss of generality, we discuss the case that a $6M\times 6N$ large image is to be rendered on $M\times N$ RGB vertical stripe panel or $M\times N$ RGBX square-shaped panel using corresponding subpixel rendering techniques.

II-A. RGB Vertical Stripe Subpixel Arrangement

Let (m_k, n_k) ($k=1,2,3$ represent R, G and B color components) be sampling locations of the RGB color components when applying $6:1$ sub-sampling on RGB vertical stripe panel, i.e., $m_k\in\{1,2,\cdots,6\}$ and $n_k\in\{1,2,\cdots,6\}$ for each 6×6 block, and

$$\begin{array}{l} R_{\text{RGB}}(i,j) = \\ \begin{cases} R(i,j), & i=6(ii-1)+m_1, j=6(jj-1)+n_1, \\ 0, & \text{otherwise;} \end{cases} \\ G_{\text{RGB}}(i,j) = \\ \begin{cases} G(i,j), & i=6(ii-1)+m_2, j=6(jj-1)+n_2, \\ 0, & \text{otherwise;} \end{cases} \\ B_{\text{RGB}}(i,j) = \\ \begin{cases} B(i,j), & i=6(ii-1)+m_3, j=6(jj-1)+n_3, \\ 0, & \text{otherwise,} \end{cases} \end{array} \tag{1}$$

where $R(i,j)$ is the red component of $6M\times 6N$ input image. (i,j) and (ii,jj) are spatial indexes of the large and small images respectively. $R_{\text{RGB}}(i,j)$ is the red component of $6M\times 6N$ pseudo image, which is sub-sampled based on RGB vertical stripe subpixel arrangement. Then the luminance component (denoted as $I(i,j)$) for the $(i,j)^{th}$ pixel of pseudo image is simply

$$\begin{aligned} I_{\text{RGB}}(i,j) &= \tfrac{1}{3}(R_{\text{RGB}}(i,j)+G_{\text{RGB}}(i,j)+B_{\text{RGB}}(i,j)) \\ &= \tfrac{1}{3}(R\Delta^R_{\text{RGB}}(i,j)+G\Delta^G_{\text{RGB}}(i,j)+B\Delta^B_{\text{RGB}}(i,j)) \\ &= \tfrac{1}{3}\sum_{k=1,2,3} C_k(i,j)\Delta^k_{\text{RGB}}(i,j), \end{aligned} \tag{2}$$

where C_k are RGB color components ($k=1,2,3$ represent R, G, and B). $\Delta^k_{\text{RGB}}(i,j)$ are RGB modulation functions determined by the sampling locations (m_k,n_k) of pseudo image, as shown in (3). The Fourier transform of I_{RGB} is

$$\widehat{I}_{\text{RGB}}(u,v) = \frac{1}{3}\sum_{k=1,2,3}\widehat{C}_k(u,v) * \widehat{\Delta}^k_{\text{RGB}}(u,v), \tag{4}$$

where $\widehat{\cdot}$ represents the Discrete Time Fourier transform and $*$ is the convolution operator. Note that the modulation function in (3) can be divided into horizontal and vertical sub-sampling separately. Without loss of generality, let us discuss the horizontal modulation function firstly, i.e.,

$$\begin{aligned} \widehat{\Delta}^k_{\text{RGB}}(u) &= \tfrac{2}{3}\left[\tfrac{1}{2}e^{-j\frac{\pi}{3}m_k}\delta(u-\tfrac{1}{6})+\tfrac{1}{2}e^{j\frac{\pi}{3}m_k}\delta(u+\tfrac{1}{6})\right] \\ &* \left[\tfrac{1}{2}e^{-j\frac{\pi}{3}m_k}\delta(u-\tfrac{1}{6})+\tfrac{1}{2}e^{j\frac{\pi}{3}m_k}\delta(u+\tfrac{1}{6})-\tfrac{1}{2}\right] \\ &* \left[\tfrac{1}{2}e^{-j\frac{\pi}{3}m_k}\delta(u-\tfrac{1}{6})+\tfrac{1}{2}e^{j\frac{\pi}{3}m_k}\delta(u+\tfrac{1}{6})+\tfrac{1}{2}\right] \\ &* \left[\tfrac{1}{2}e^{-j\frac{\pi}{3}m_k}\delta(u-\tfrac{1}{6})+\tfrac{1}{2}e^{j\frac{\pi}{3}m_k}\delta(u+\tfrac{1}{6})+1\right]. \end{aligned} \tag{5}$$

Similarly, we have $\widehat{\Delta}^k_{\text{RGB}}(v)$. Let $p_k = e^{j\frac{\pi}{3}m_k}$ and $q_k = e^{j\frac{\pi}{3}n_k}$, then $p_k^* = e^{-j\frac{\pi}{3}m_k}$ and $q_k^* = e^{-j\frac{\pi}{3}n_k}$. We have

$$\widehat{\Delta}^k_{\text{RGB}}(u,v) = \mathbf{\Delta}(\mathbf{u})^T \begin{bmatrix} p_kq_k & p_k & p_kq_k^* \\ q_k & 1 & q_k^* \\ p_k^*q_k & p_k^* & p_k^*q_k^* \end{bmatrix} \mathbf{\Delta}(\mathbf{v}), \tag{6}$$

where $\mathbf{\Delta}(\mathbf{u}) = [\delta(u+\frac{1}{6}), \delta(u), \delta(u-\frac{1}{6})]^T$ and $\mathbf{\Delta}(\mathbf{v}) = [\delta(v+\frac{1}{6}), \delta(v), \delta(v-\frac{1}{6})]^T$, and $[\cdot]^T$ denotes transposition. Substitute $\widehat{\Delta}^k_{\text{RGB}}(u,v)$ in (4) with (6), we have

$$\begin{aligned} &\widehat{I}_{\text{RGB}}(u,v) = \\ &\mathbf{1}_3^T \begin{bmatrix} \widehat{C}_{pq}(u^+,v^+) & \widehat{C}_p(u^+,v) & \widehat{C}_{pq^*}(u^+,v^-) \\ \widehat{C}_q(u,v^+) & \widehat{I}_0(u,v) & \widehat{C}_q^*(u,v^-) \\ \widehat{C}_{pq^*}^*(u^-,v^+) & \widehat{C}_p^*(u^-,v) & \widehat{C}_{pq}^*(u^-,v^-) \end{bmatrix} \mathbf{1}_3, \end{aligned} \tag{7}$$

where $u^\pm = u\pm\frac{1}{6}$, $v^\pm = u\pm\frac{1}{6}$. $\widehat{I}_0(u,v)$ is the luminance component of original input image, $\widehat{I}_0 = \frac{1}{3}(\widehat{R}+\widehat{G}+\widehat{B})$. C_p, C_q, C_{pq^*} and C_{pq} are linear combinations of RGB color components,

$$\begin{aligned} \widehat{C}_p(u,v) &= \tfrac{1}{3}(p_1\widehat{R}(u,v)+p_2\widehat{G}(u,v)+p_3\widehat{B}(u,v)) \\ \widehat{C}_q(u,v) &= \tfrac{1}{3}(q_1\widehat{R}(u,v)+q_2\widehat{G}(u,v)+q_3\widehat{B}(u,v)) \\ \widehat{C}_{pq^*}(u,v) &= \tfrac{1}{3}(p_1q_1^*\widehat{R}(u,v)+p_2q_2^*\widehat{G}(u,v)+p_3q_3^*\widehat{B}(u,v)) \\ \widehat{C}_{pq}(u,v) &= \tfrac{1}{3}(p_1q_1\widehat{R}(u,v)+p_2q_2\widehat{G}(u,v)+p_3q_3\widehat{B}(u,v)). \end{aligned} \tag{8}$$

$$\begin{aligned}\Delta^k_{\mathrm{RGB}}(i,j) &= \Delta^k_{\mathrm{RGB}}(i) \times \Delta^k_{\mathrm{RGB}}(j) \\ &= \left[\tfrac{2}{3}\cos\tfrac{\pi(i-m_k)}{3}(\cos\tfrac{\pi(i-m_k)}{3}-\tfrac{1}{2})(\cos\tfrac{\pi(i-m_k)}{3}+\tfrac{1}{2})(\cos\tfrac{\pi(i-m_k)}{3}+1)\right] \\ &\times \left[\tfrac{2}{3}\cos\tfrac{\pi(j-n_k)}{3}(\cos\tfrac{\pi(j-n_k)}{3}-\tfrac{1}{2})(\cos\tfrac{\pi(j-n_k)}{3}+\tfrac{1}{2})(\cos\tfrac{\pi(j-n_k)}{3}+1)\right]\end{aligned} \tag{3}$$

Each color component such as $\widehat{R}$ can be decomposed into a low-frequency term $\widehat{R}_l$ and a high frequency term $\widehat{R}_h$, i.e, $\widehat{R} = \widehat{R}_l + \widehat{R}_h$, and since the high frequency components of different colors tend to be similar [7] [8] [9], i.e. $\widehat{R}_h(u,v) \approx \widehat{G}_h(u,v) \approx \widehat{B}_h(u,v)$, we have

$$\begin{aligned}&\widehat{C}_p(u,v) = \tfrac{1}{3}(p_1\widehat{R}(u,v) + p_2\widehat{G}(u,v) + p_3\widehat{B}(u,v)) \\ &= \tfrac{1}{3}\left[(p_1\widehat{R}_l + p_2\widehat{G}_l + p_2\widehat{B}_l) + (p_1\widehat{R}_h + p_2\widehat{G}_h + p_3\widehat{B}_h)\right] \\ &\approx \tfrac{1}{3}\left[(p_1\widehat{R}_l + p_2\widehat{G}_l + p_2\widehat{B}_l) + (p_1+p_2+p_3)\widehat{B}_h)\right].\end{aligned} \tag{9}$$

Examining (9), $\widehat{C}_p$ would be mainly composed by low frequency signal if $p_1 + p_2 + p_3 = 0$. Similar argument is addressed for $\widehat{C}_q$ to achieve $q_1 + q_2 + q_3 = 0$. In other words, by choosing appropriate m_k and n_k, the magnitudes of horizontal and vertical aliasing spectra $|\widehat{C}_p|$ and $|\widehat{C}_q|$ can be minimized to be $|\widehat{C}_p| \approx |\frac{1}{3}(p_1\widehat{R}_l + p_2\widehat{G}_l + p_2\widehat{B}_l)|$ and $|\widehat{C}_q| \approx |\frac{1}{3}(q_1\widehat{R}_l + q_2\widehat{G}_l + q_2\widehat{B}_l)|$. To achieve $p_1+p_2+p_3 = 0$, where $p_k = e^{j\frac{\pi}{3}m_k}$ and $m_k \in \{1,2,\cdots,6\}$, the solution m_k is the set of $\{1,3,5\}$ or $\{2,4,6\}$. While for n_k, due to RGB subpixel arrangement in RGB vertical stripe panel (i.e., $n_1 \le n_2 \le n_3$), the solution is $n_3 = n_2 + 2 = n_1 + 4$. Then $(n_1, n_2, n_3) = (1,3,5)$ or $(2,4,6)$, as shown in Fig. 3(a).

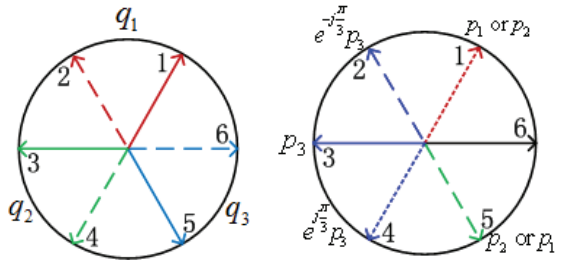

(a) (b)

Fig. 3. (a) The solution of $\sum_{k=1}^{3} q_k = 0$ is $(n_1, n_2, n_3) = (1,3,5)$ or $(2,4,6)$, $k = 1,2,3$ represent R, G and B color components. (b) Example of the solution to (11).

Under the constraints of $\sum_{k=1}^{3} p_k = 0$ and $\sum_{k=1}^{3} q_k = 0$, we would like to further minimize the magnitudes of replicated spectra in diagonal direction ($|\widehat{C}_{pq}|$) and anti-diagonal direction ($|\widehat{C}_{pq^*}|$), which are mainly determined by the magnitudes of high-frequency terms,

$$\begin{aligned}\min_{m_k} \quad & |\sum_{k=1}^{3} p_k q_k| + |\sum_{k=1}^{3} p_k q_k^*| \\ \text{s.t.} \quad & \sum_{k=1}^{3} p_k = 0 \\ & p_k = e^{j\frac{\pi}{3}m_k} \\ & q_3 = e^{j\frac{2\pi}{3}} q_2 = e^{j\frac{4\pi}{3}} q_1 \\ & m_k \in \{1,2,\cdots,6\}.\end{aligned} \tag{10}$$

Rewriting (10) by substituting p_k and q_k with constraints,

$$\begin{aligned}\min_{m_k} \quad & |p_2 + e^{j\frac{\pi}{3}}p_3| + |p_2 + e^{-j\frac{\pi}{3}}p_3| \\ \text{s.t.} \quad & p_k = e^{j\frac{\pi}{3}m_k} \\ & m_k \in \{1,2,\cdots,6\}.\end{aligned} \tag{11}$$

Fig. 3(b) depicts an example of the solution to (11), where the values of m_1, m_2 and m_3 follow clockwise $m_3 = m_2 + 2 = m_1 + 4$ or anti-clockwise $m_1 = m_2 + 2 = m_3 + 4$. These two cases lead to $|\sum_{k=1}^{3} p_k q_k| = 0$ or $|\sum_{k=1}^{3} p_k q_k^*| = 0$ respectively. However, $|\sum_{k=1}^{3} p_k q_k| = 0$ and $|\sum_{k=1}^{3} p_k q_k^*| = 0$ can never be achieved simultaneously. In conclusion, the horizontal and vertical replicated spectra $\widehat{C}_p$ and $\widehat{C}_q$ will merely contain low-frequency information by choosing appropriate m_k and n_k, which means that the horizontal and vertical cut-off frequency of subpixel-based down-sampling for RGB stripe panel can be effectively extended beyond Nyquist cut-off frequency, so that to retain more original high frequency information. While the diagonal and anti-diagonal replicated spectra $\widehat{C}_{pq}$ and $\widehat{C}_{pq^*}$ can not simultaneously suppress their high frequency information in any case, which is the limitation of RGB vertical stripe subpixel arrangement.

II-B. RGBX Square-shaped Subpixel Arrangement

The luminance component of the pseudo image that down-sampled based on RGBX square-shaped subpixel arrangement is similar to (7), except that $\widehat{I}_0$, C_p, C_q, C_{pq^*} and C_{pq} are linear combinations of RGBX four color components. Following the same argument as (9), the horizontal and vertical replicated aliasing spectra ($\widehat{C}_p$ and $\widehat{C}_q$) would be mainly composed by low frequency signal if $p_1 + p_2 + p_3 + p_4 = 0$ and $q_1 + q_2 + q_3 + q_4 = 0$, where $p_k = e^{j\frac{\pi}{3}m_k}$, $q_k = e^{j\frac{\pi}{3}n_k}$. Due to the subpixel arrangement in RGBX square-shaped panel in Fig. 2(b), the sampling locations of RGBX four color components belong to the sets $m_1 \in \{1,2,3\}$, $n_1 \in \{4,5,6\}$, $m_2 \in \{1,2,3\}$, $n_2 \in \{1,2,3\}$, $m_3 \in \{4,5,6\}$, $n_2 \in \{1,2,3\}$, and $m_4 \in \{4,5,6\}$, $n_4 \in \{4,5,6\}$ respectively. Fig. 4 depicts the choice of (m_k, n_k) to achieve

$\sum_{k=1}^{4} p_k = 0$ and $\sum_{k=1}^{4} q_k = 0$, where $p_3 = -p_1$, $p_4 = -p_2$ ($m_3 = m_1 + 3, m_4 = m_2 + 3$), or $p_3 = -p_2$, $p_4 = -p_1$ ($m_3 = m_2 + 3, m_4 = m_3 + 3$). Similarly, $q_1 = -q_2$, $q_4 = -q_3$ ($n_1 = n_2 + 3, n_4 = n_3 + 3$), or $q_1 = -q_3$, $q_4 = -q_2$ ($n_1 = n_3 + 3, n_4 = n_2 + 3$). Without loss of generality, we discuss the case $p_3 = -p_1$ and $q_1 = -q_2$. The other cases lead to the same conclusion.

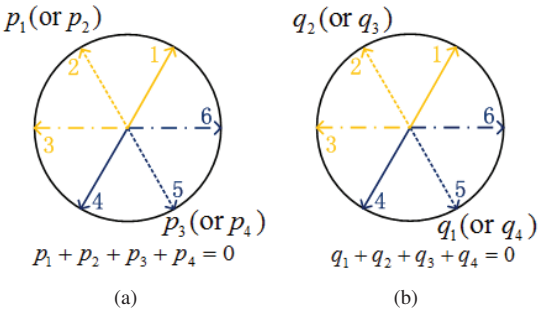

Fig. 4. Example of solutions to $\sum_{k=1}^{4} p_k = 0$ and $\sum_{k=1}^{4} q_k = 0$.

To minimize the magnitudes of replicated spectra in diagonal direction ($|\widehat{C}_{pq}|$) and anti-diagonal direction ($|\widehat{C}_{pq^*}|$),

$$\begin{aligned} \min_{m_k, n_k} \quad & |\sum_{k=1}^{4} p_k q_k| + |\sum_{k=1}^{4} p_k q_k^*| \\ s.t. \quad & p_k = e^{j\frac{\pi}{3}m_k}, q_k = e^{j\frac{\pi}{3}n_k}, \\ & p_3 = -p_1, p_4 = -p_2, \text{ or } p_3 = -p_2, p_4 = -p_1, \\ & q_1 = -q_2, q_4 = -q_3, \text{ or } q_1 = -q_3, q_4 = -q_2, \\ & m_1, m_2, n_2, n_3 \in \{1, 2, 3\} \end{aligned} \tag{12}$$

It can be shown that the optimal solution of (12) is $m_3 = m_4 = m_1 + 3 = m_2 + 3$ and $n_1 = n_4 = n_2 + 3 = n_3 + 3$, which achieves both $|\sum_{k=1}^{4} p_k q_k| = 0$ and $|\sum_{k=1}^{4} p_k q_k^*| = 0$ simultaneously, indicating that both diagonal and anti-diagonal replicated aliasing spectra ($\widehat{C}_{pq}$ and $\widehat{C}_{pq^*}$) merely contain low-frequency information, results in relatively compact spectra.

Recall that subpixel-based down-sampling on traditional RGB vertical stripe panel achieves higher apparent resolution than pixel-based down-sampling due to the small magnitudes of horizontal and vertical aliasing spectra. Thanks to the 2-D RGBX square-shaped subpixel arrangement, all the horizontal, vertical, diagonal and anti-diagonal aliasing spectra merely contains low-frequency terms, leading to small magnitudes of all the aliasing spectra. In other words, under the same sub-sampling ratio, subpixel-based down-sampling with RGBX square-shaped panel will have superior performance than RGB vertical stripe subpixel arrangement, to retain more original high frequency details.

III. CONCLUSION

In this paper, we study the frequency behavior of RGB vertical stripe and RGBX square-shaped subpixel arrangements respectively. Our frequency analysis shows that subpixel-based down-sampling with RGBX square-shaped subpixel arrangement is more effective in retaining original high frequency details than RGB vertical stripe subpixel arrangement due to the smaller magnitudes of replicated aliasing spectra in both diagonal and anti-diagonal direction.

IV. ACKNOWLEDGMENT

This work has been supported in part by the Research Grants Council (RGC) of the Hong Kong Special Administrative Region, China. (GRF 610109), the Shanghai Pujiang Program under Grant 11PJ1409400 and the National Natural Science Foundation of China under Grant 61102059.

V. REFERENCES

[1] "ClearType information", *from http://www.microsoft.com/typography/cleartypeinfo.mspx*.
[2] S. Gibson, "Sub-pixel font rendering technology", *from http://www. grc. com/cleartype. htm.*
[3] J. C. Platt, "Optimal filtering for patterned displays", *IEEE SPL*, pp. 179-181, vol. 7, no. 7, 2000.
[4] S. Daly, "Analysis of subtriad addressing algorithms by visual system models", *SID Int. Symp. Digest of Technical Papers*, pp. 1200-1204, vol. 32, 2001.
[5] T. L. Credelle, C. B. Elliott, M. F. Higgins, "P-00: MTF of High-Resolution PenTile Matrix Displays", ClairVoyante Laboratories, Sebastopol, CA, USA 707-824-2060, *tcredelle@clairvoyante.com*.
[6] "Virtual Resolution Banishes Pixel Limits in Mobile Displays", *www.vp-dynamics.com*.
[7] L. Fang, O. C. Au, K. Tang, A. K. Katsaggelos, "Anti-aliasing Filter Design for Subpixel Down-sampling via Frequency Domain Analysis", *IEEE Trans. on Image Processing*, vol. 21, No. 3, pp. 1391-1405, Mar. 2012.
[8] K. Hirakawa, P. J. Wolfe, "Spatio-spectral Color Filter Array Design for Optimal Image Recovery", *IEEE Trans. on Image Processing*, vol. 17, No. 10, pp. 1876-1890, Oct. 2008.
[9] D. Alleysson, S. Susstrunk, and J. Herault, "Linear Demosaicing Inspired by the Human Visual System", *IEEE Trans. on Image Processing*, vol. 14, No. 4, pp. 439-449, April 2005.